Received: 29 March 2016 | Revised: 30 May 2016 | Accepted: 25 June 2016

DOI 10.1002/bip.22898

REVIEW

WILEY PeptideScience

Oxazolidinone-containing pseudopeptides: supramolecular materials, fibers, crystals, and gels

Claudia Tomasini | Nicola Zanna

Dipartimento Di Chimica Ciamician, Università Di Bologna, via Selmi, 2, Bologna 40137, Italy

Correspondence
Prof. Claudia Tomasini, Dipartimento di Chimica Ciamician, Università di Bologna, via Selmi, 2, Bologna 40137, Italy.
Email: claudia.tomasini@unibo.it

Abstract

The formation of fibers through self-assembly is of particular interest, as fibrous proteins (such as collagen, keratin, actin, and so on) are involved in intra- and extracellular functions. To understand aggregation phenomena, oligopeptides may be designed and prepared either to mimic or to interfere with these processes. In this article, we will demonstrate that the introduction of the 4-methyl-5-carboxy-oxazolidin-2-one (Oxd) moiety inside a peptide chain favors the formation of fiber-like materials organized either in β-sheets or in supramolecular helices, provided that it is combined with other factors, like π-stacking interactions and intermolecular N—H···O═C bonds. The presence of the Oxd moiety is essential for the material formation: when Oxd is replaced with Pro, only liquids or amorphous solids are obtained. Remarkably, some of these molecules are low-molecular-weight gelators, as they induce the formation of both organogel and hydrogels that have been used for several applications.

KEYWORDS
fiber-like material, gelators, gels, pseudopeptides, supramolecular material

1 | INTRODUCTION

Aggregation and disaggregation are central phenomena in nature.[1] In this context, the formation of fibers through self-assembly is of particular interest, as fibrous proteins (such as collagen, keratin, actin, and so on) are involved in intra- and extracellular functions.[2,3] The comprehension of the mechanism adopted by short oligomers that form fibers and fibrils may help in the understanding of neurodegenerative diseases development, such as Alzheimer's disease,[4] diabetes,[5] scrapie (in sheep),[6] BSE (in cattle),[7] and Creutzfeld-Jakob's disease (in humans).[8] All these illnesses are induced by amyloid peptides that adopt a β-sheet conformation that favors the aggregation in the extracellular space.[9] This process is thermodynamically favorable as β-sheet layers are the most stable proteinaceous superstructure in nature.[10]

To understand aggregation phenomena, oligopeptides may be designed and prepared either to mimicking[11–16] or to interfere with[17–19] these processes. Indeed, the potential applications of such supramolecular assemblies exceed those of synthetic polymers since the building blocks may introduce biological functions in addition to mechanical properties.[20]

Nearly 10 years ago we found out that our 4-methyl-5-carboxy-oxazolidin-2-one moiety (that we will call Oxd from now on) could be successfully utilized in the formation of supramolecular materials. This little molecule, that mimics a proline group, may form oligomers having stable secondary structures in solution, due to its ability to block the peptide bond always in the *trans* conformation.[21–23] This outcome does not take place in the prolyl bonds that can also adopt the *cis* conformation.[24–28]

This property induces a local constraint in the pseudopeptide chain that may cause the formation of supramolecular materials, provided that it is combined with other factors, like π-stacking interactions and intermolecular N—H···O═C bonds. Thus the L-Phe-D-Oxd (L-Phe = L-phenylalanine) moiety displays all these effects and may be considered a privileged scaffold for the formation of supramolecular materials (Figure 1).

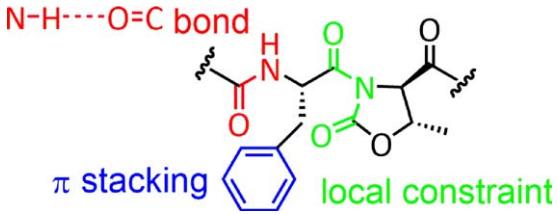

FIGURE 1 Chemical structure of the L-Phe-D-Oxd moiety that is a privileged structure for the formation of supramolecular materials

This review article is a critical overview of a variety of Oxd-containing pseudopeptides which are able to form fibers and supramolecular helices. Some derivatives are able to form gels, so we report their applications as low-molecular-weight gelators (LMWG), focusing our attention on the importance of the Oxd moiety for the formation of these supramolecular structures.

2 | FIBER-LIKE MATERIALS

2.1 | L-Phe-D-Oxd containing fiber-like materials

The first example of a molecule containing the L-Phe-D-Oxd moiety and able to form a supramolecular material is Boc-L-Phe-D-Oxd-OBn **1**.[29] After overnight evaporation of a 25 mM solution containing the pseudopeptide in a 1:1 mixture of cyclohexane and ethyl acetate, the white solid shown in Figure 2A is formed. This fiber-like material is stabilized only by single hydrogen bonds between dipeptide units, as demonstrated by the X-ray crystal structure reported in Figure 2B. Such an assembly represents the absolute borderline case of a sheet structure, as the second amino acid of the dipeptide is not involved in further intermolecular interactions.

Given these results that clearly demonstrate the importance of a phenyl ring in the backbone, Boc-L-Phe-D-Pro-OBn **2** was prepared, replacing the D-Oxd moiety with a D-Pro (D-Pro = D-proline) unit, to check if the presence of the Oxd moiety is essential for the formation of the supramolecular material. In contrast with the behavior of **1**, no material is even obtained with **2**, that is a colorless liquid (Figure 3).

This outcome suggests that the L-Phe-D-Oxd moiety is essential for the formation of supramolecular materials and may be used to induce selected properties in the solid state. So a series of oligomers containing several L-Phe-D-Oxd units was prepared using liquid phase conditions.[30] While Boc-(L-Phe-D-Oxd)$_2$-OBn **3** forms a fiber-like material with an antiparallel β-sheet structure where the oligopeptide units are connected by only one intermolecular hydrogen bond (an SEM image and the X-ray crystal structure of **3** are shown in Figure 4), the longer oligomers Boc-(L-Phe-D-Oxd)$_n$-OBn (n = 3–5) get organized in helices by formation of intramolecular hydrogen bonds that prevent the formation both of intermolecular hydrogen bonds and of fibers.

Much to our surprise, the epimeric oligomer Boc-(L-Phe-L-Oxd)$_2$-OBn **4** cannot form supramolecular materials on its own, as it forms amorphous solids in any crystallization condition. Interestingly very nice crystals suitable for X-ray diffraction study were obtained on slow evaporation of a 1:1 diastereoisomeric mixture of Boc-(L-Phe-L-Oxd)$_2$-OBn **4** and Boc-L-Phe-L-Oxd-D-Phe-L-Oxd-OBn **5** in methyl *t*-butyl ether. The preferential conformation of both oligomers was fully elucidated in the solid phase and the X-ray crystal structures of the two epimers are shown in Figure 5.[31]

The preferred conformation of Boc-(L-Phe-L-Oxd)$_2$-OBn **4** ranges between a PPII helix and a β-strand, while the previously reported Boc-(L-Phe-D-Oxd)$_2$-OBn **3** forms infinite antiparallel β−sheet structures (Figure 4), thus showing that the absolute

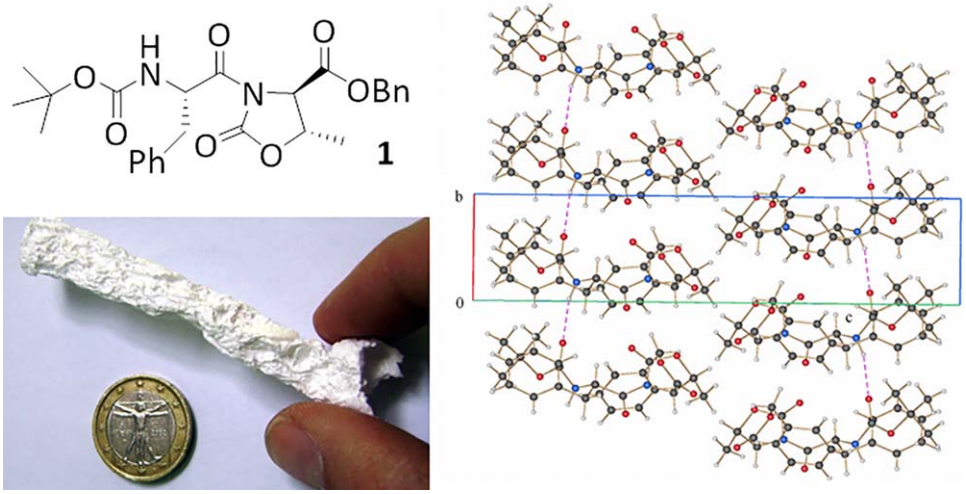

FIGURE 2 (A) String of pure Boc-L-Phe-D-Oxd-OBn **1** obtained after slow evaporation of the solvent from a 25 mM solution. (B) Crystal packing showing one chain running along the *b* axis generated by a single N—H···O═C interaction between the molecules. Reproduced from Ref. 29 with permission from Wiley-VCH

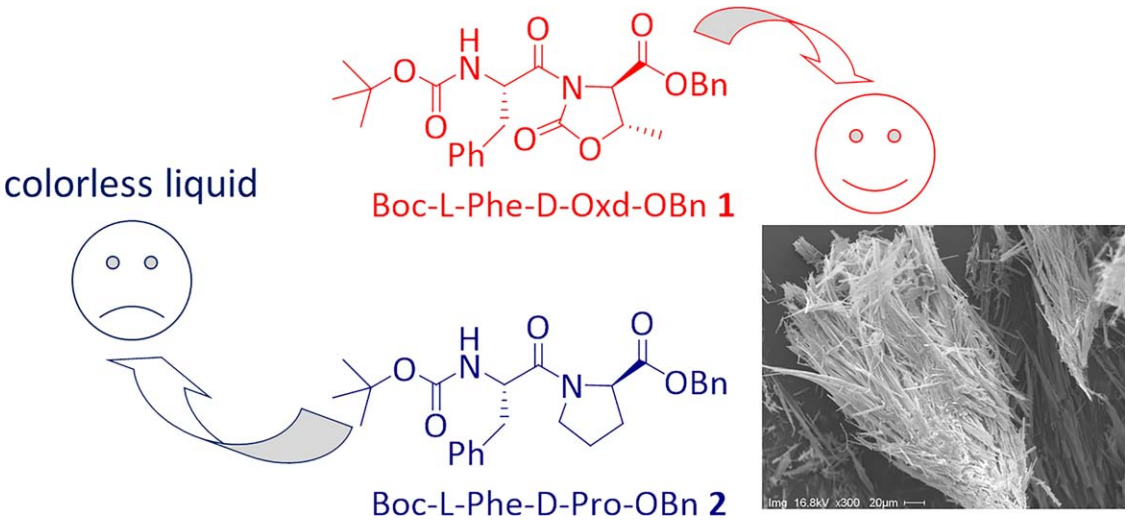

FIGURE 3 Comparison between the behaviors of Boc-L-Phe-D-Oxd-OBn **1** and Boc-L-Phe-D-Pro-OBn **2**

configuration reversal of the Oxd moieties has a strong effect on the secondary structure of these oligomers. The same outcome was retained in solution, as demonstrated by vibrational circular dichroism (VCD) analysis coupled with DFT calculations.

If another crystallization solvent is used, the 1:1 epimeric mixture of Boc-(L-Phe-L-Oxd)$_2$-OBn **4** and Boc-L-Phe-L-Oxd-D-Phe-L-Oxd-OBn **5** leads to the formation of other materials, such as crystals, fibers and globules, that are shown in Figure 6.

The precipitates from diethyl ether and methyl *t*-butyl ether are formed by aggregates of plate-like crystals having a variable area and thickness that ranges from 1 to 5 μm. In contrast, the mixture precipitated from isopropanol shows a fibrous structure, while the one precipitated from methanol forms regular globular shapes that are unstable under the electron beam generating a rough surface, thus suggesting that these globes contain methanol that quickly evaporates if the sample is heated.

2.2 | Derivatives of the L-Phe-D-Oxd moiety leading to fiber-like materials

The L-Phe-D-Oxd moiety may be further derivatized without losing its tendency to form supramolecular materials: the tripeptide Boc-(L-Phe)$_2$-D-Oxd-OBn **6** was prepared to check if it behaves like **1**[32] or like Phe–Phe, that forms nanotubes in the solid state.[33] Figure 7 shows the X-ray crystal structure of **6** that forms parallel β-sheet structure where the oligopeptide units are connected by two intermolecular hydrogen bonds. This structure resembles **1**, thus demonstrating that molecules containing one or two Phe residues show the same behavior in solid.

Then the two epimers Boc-L-Phe-D-Oxd-(*S*)-β^3-*h*Phg-OBn **7** and Boc-L-Phe-D-Oxd-(*R*)-β^3-*h*Phg-OBn **8** have been prepared by standard methods in solution, coupling β^3-*h*Phg-OH in both enantiomeric forms to the L-Phe-D-Oxd moiety. The conformation of **7** and **8** was analyzed both in solution

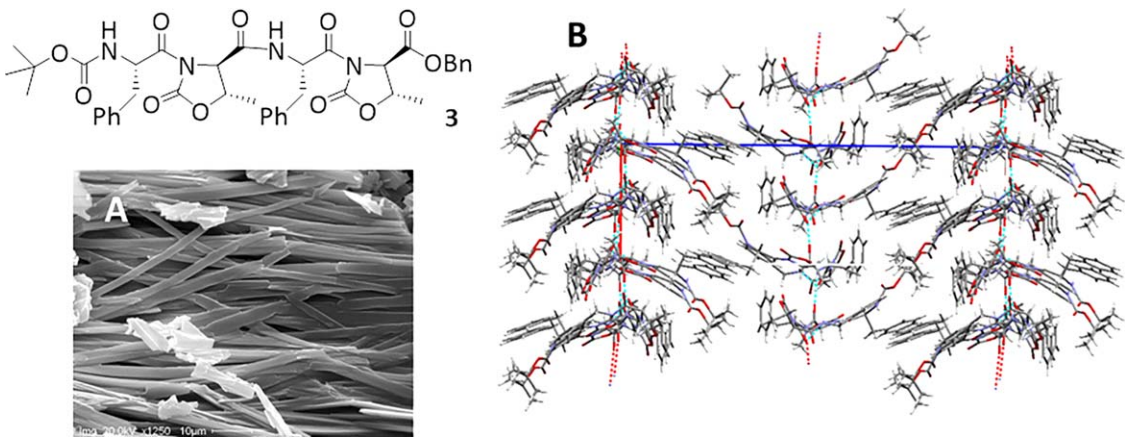

FIGURE 4 (A) An SEM picture of Boc-(L-Phe-D-Oxd)$_2$-OBn **3**; (B) view down the crystallographic *b* axis of the crystal packing of Boc-(L-Phe-D-Oxd)$_2$-OBn **3** showing the intermolecular NH. . .CO hydrogen bond running along the *a* axis. Reproduced from Ref. 30 with permission from Wiley-VCH

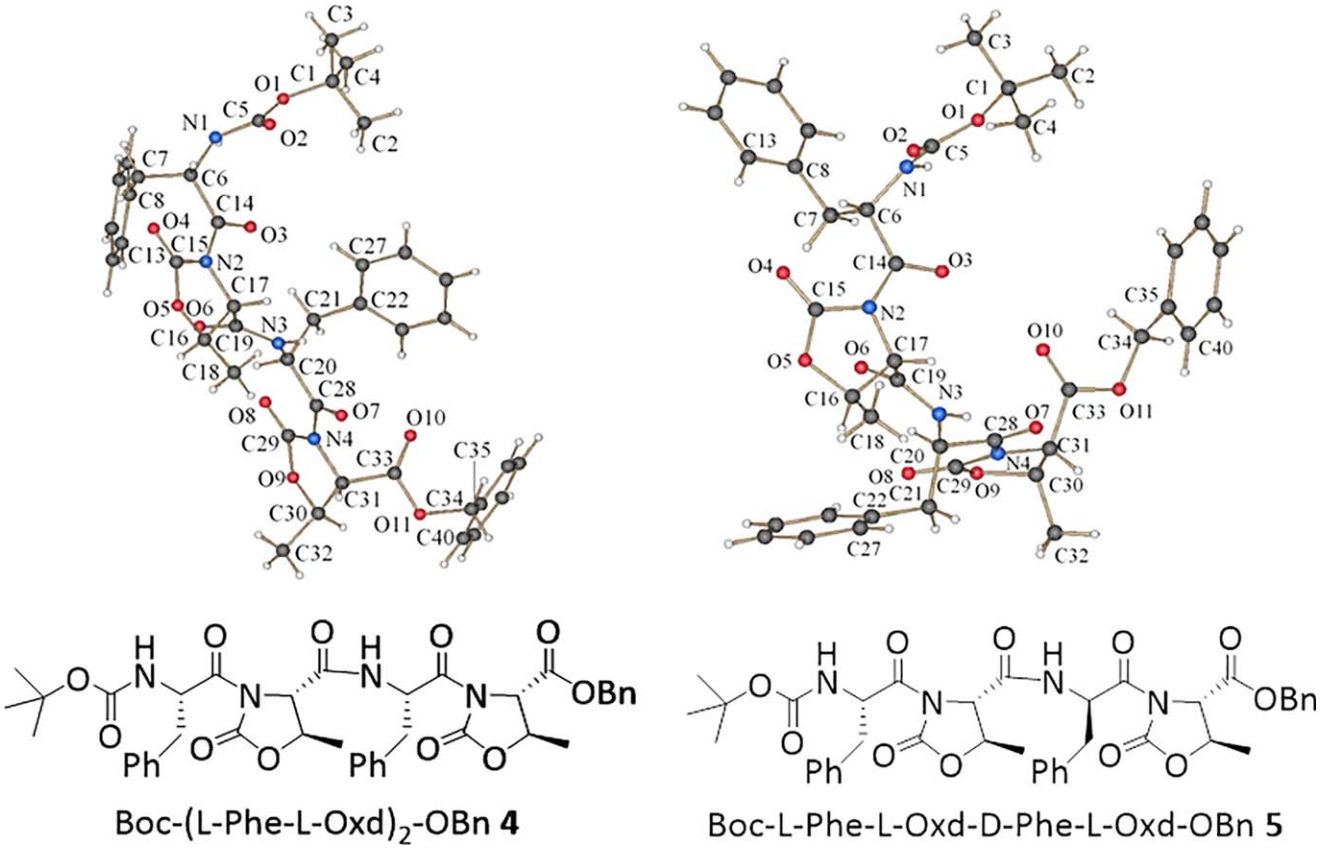

FIGURE 5 Crystal structure of Boc-(L-Phe-L-Oxd)$_2$-OBn **4** and Boc-L-Phe-L-Oxd-D-Phe-L-Oxd-OBn **5**. Reproduced from Ref. 31 with permission from Wiley-VCH

and in the solid state[34]: while in solution Boc-L-Phe-D-Oxd-(*S*)-β^3-*h*Phg-OBn **7** shows a random coil structure, **8** tends to assume a γ-turn conformation that is nearly retained in the solid state. In both cases, crystals are obtained, rather than fiber-like materials, but the reversal of the stereogenic center absolute configuration of the *h*Phg moiety produces a different crystal morphology due to a different crystal packing. Molecules of **7** associate in the solid state, generating a helix

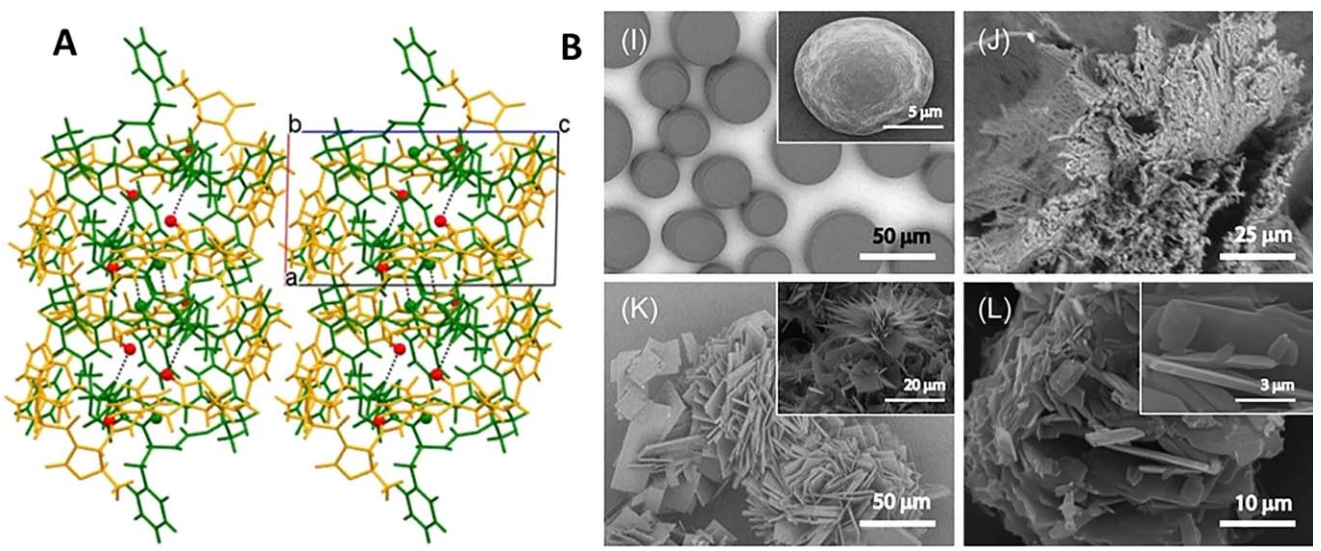

FIGURE 6 (A) Perspective view of the crystal packing of the epimeric pair of Boc-(L-Phe-L-Oxd)$_2$-OBn **4** and Boc-L-Phe-L-Oxd-D-Phe-L-Oxd-OBn **5** showing two of the columns running along the *a* axis (the solvent molecules are not represented for the sake of clarity); (B) SEM pictures of the epimeric mixture precipitated from methanol (**I**), isopropanol (**J**), diethyl ether (**K**), or methyl *t*-butyl ether (**L**). The insets report high magnification of details. Reproduced from Ref. 31 with permission from Wiley-VCH

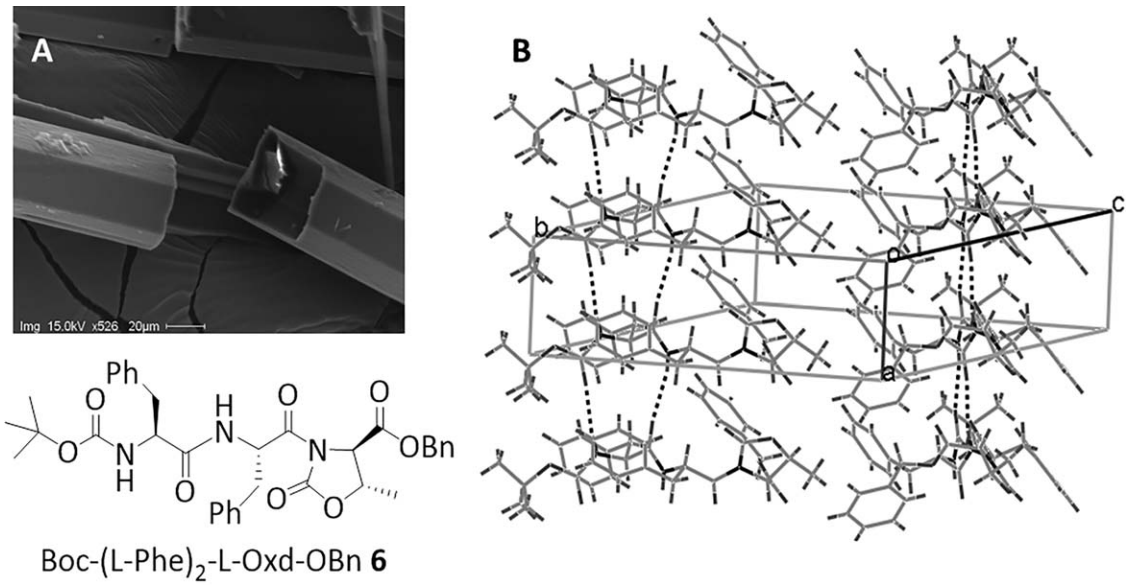

FIGURE 7 (A) SEM images of Boc-(L-Phe)$_2$-D-Oxd-OBn **6**; (B) X-ray molecular structure and crystal packing of Boc-(L-Phe)$_2$-D-Oxd-OBn **6**. Reproduced from Ref. 32 with permission from Wiley-VCH

that involves the formation of elongated crystals with hexagonal cross-section. This effect is not observed in the crystals formed by Boc-L-Phe-D-Oxd-(*R*)-β^3-hPhg-OBn **8** that forms a 1D H-bonded polymer of tape that crystallizes in different polymorphs, depending on the evaporation solvent. In Figure 8, some pictures of the crystals obtained by crystallization of **7** (Figures 8A and 8B) and 8 (Figures 8C and 8D) are shown, together with their chemical structures.

The crystal packing of **7** therefore consists of parallel chains with a helical arrangement (Figure 9) running along the *c*-axis. The formation of a ternary helix[35] in the solid state is in agreement with the SEM analysis as the crystals of **7** from methanol appear elongated in one direction with a hexagonal cross-section (Figure 8c).

3 | LOW-MOLECULAR-WEIGHT GELATORS

Gels may be divided into chemical gels and physical gels: the internal structure of chemical gels is made of chemical

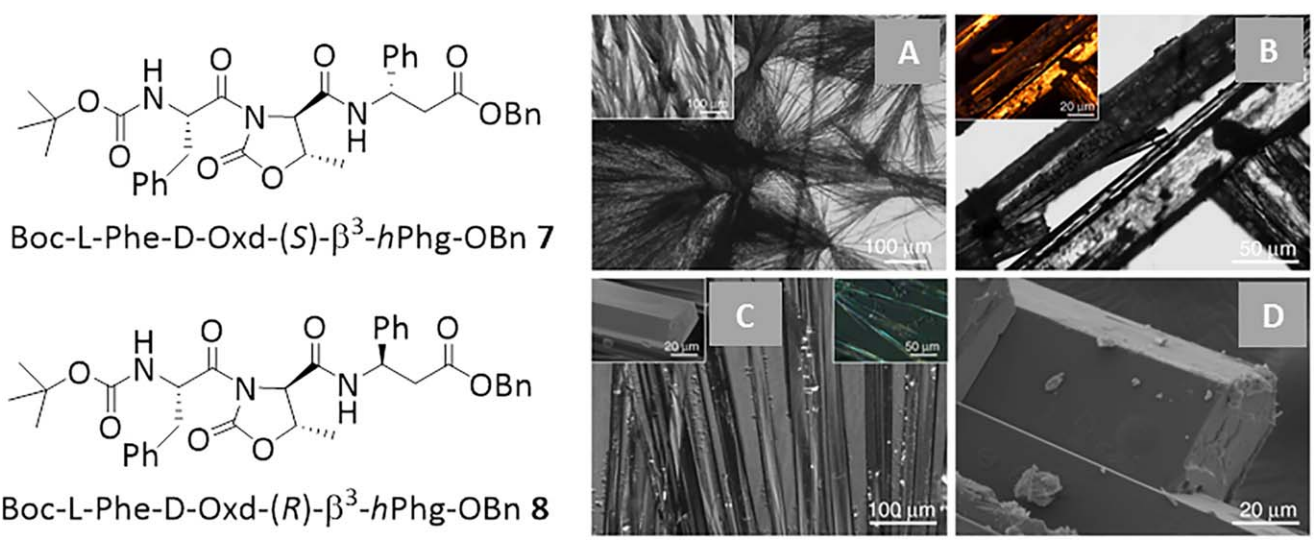

FIGURE 8 (A) Optical micrographs of Boc-L-Phe-D-Oxd-(*S*)-β^3-*h*Phg-OBn **7** precipitated from cyclohexane/ethyl acetate. The elongated growth of the crystal is observable together with their high lateral aggregation. (C) Single crystals of Boc-L-Phe-D-Oxd-(*S*)-β^3-*h*Phg-OBn **7** precipitated from ethanol, they are birefrangent and have a hexagonal cross-section. (B) and (D) crystals of Boc-L-Phe-D-Oxd-(*R*)-β^3-*h*Phg-OBn **8** precipitated from ethanol observed by means of an optical and an electron microscope, respectively. Reproduced from Ref. 34 with permission from the American Chemical Society

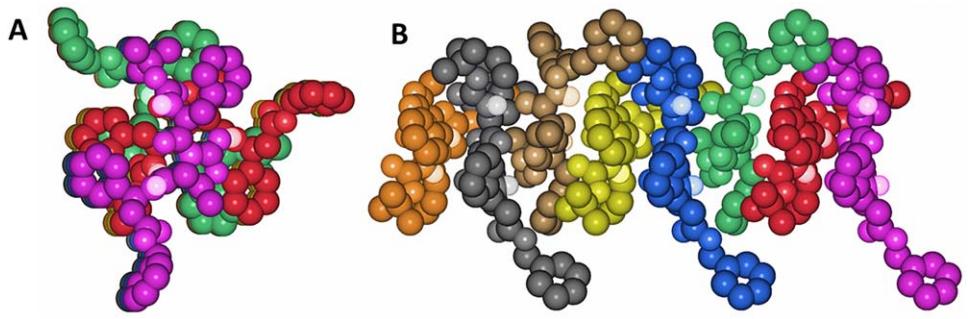

FIGURE 9 Space filling model showing the helical arrangement of one of the chains of Boc-L-Phe-D-Oxd-(*S*)-β^3-*h*Phg-OBn **7**: (A) top view, (B) view along the *c*-axis. The molecules are represented in different colors for clarity. The hydrogen atoms involved in N—H···CO hydrogen bonds are represented as white cups. Reproduced from Ref. 34 with permission from the American Chemical Society

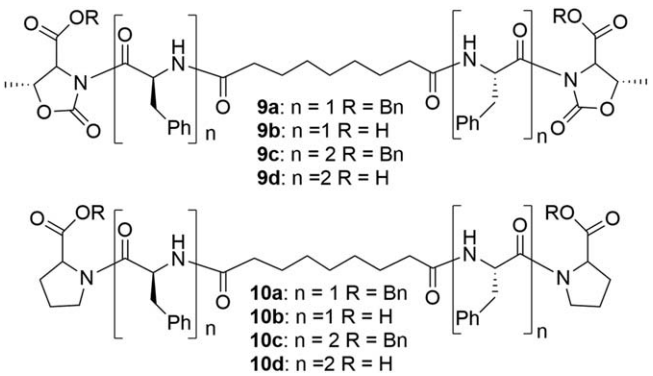

FIGURE 10 General molecular structure of bolaamphiphilic derivatives.

bonds, while physical gels are characterized by dynamic cross-links that are constantly created and broken.[36–39] The molecule able to form physical gels may be an inorganic or an organic compound, the latter having a molecular weight usually ≤500 Dalton. These compounds are generally called "low-molecular-weight gelators" (LMWGs).[40] The mechanism through which LMWGs operate depends on a hierarchical self-assembly process which occurs through the following sequence of steps: (i) multiple noncovalent interactions (eg, hydrogen bonds, π−π interactions, Van der Waals interactions) between molecular scale building blocks allow them to self-assemble into supramolecular fibrils; (ii) the fibrils often assemble into nanoscale bundles, called fibers; (iii) the fibers tangle and interact with one another to form a self-supporting, sample-spanning "solid-like" network, which underpins the macroscopic gel.[41,42]

3.1 | Bolamphiphilic LMWGs

Three factors can favor the formation of a gel: (i) the presence of hydrogen bonding and π–π stacking interactions, which are the principle interactions involved in gel aggregation; (ii) the tendency of the molecule head to organize into a network, that influences the gel formation; (iii) the presence of a long aliphatic chain connected with a polar head, such as cholesteric acids. Following these guidelines, compounds **9a–d** have been prepared by derivatization of the L-Phe-D-Oxd moiety with azelaic acid [HOOC-$(CH_2)_7$-COOH], a long chain dicarboxylic acid (Figure 10).[32] These molecules may be defined as synthetic "bolaamphiphiles."[43] Four

FIGURE 11 (A) Photograph of a gel obtained with a 10 mM solution of BnO-D-Oxd-L-Phe-OOC-$(CH_2)_7$-COO-L-Phe-D-Oxd-OBn **9a** in a 1:1 mixture of dichloromethane and ethyl acetate; (B) OM image of the same sample. Reproduced from Ref. 32 with permission from Wiley-VCH

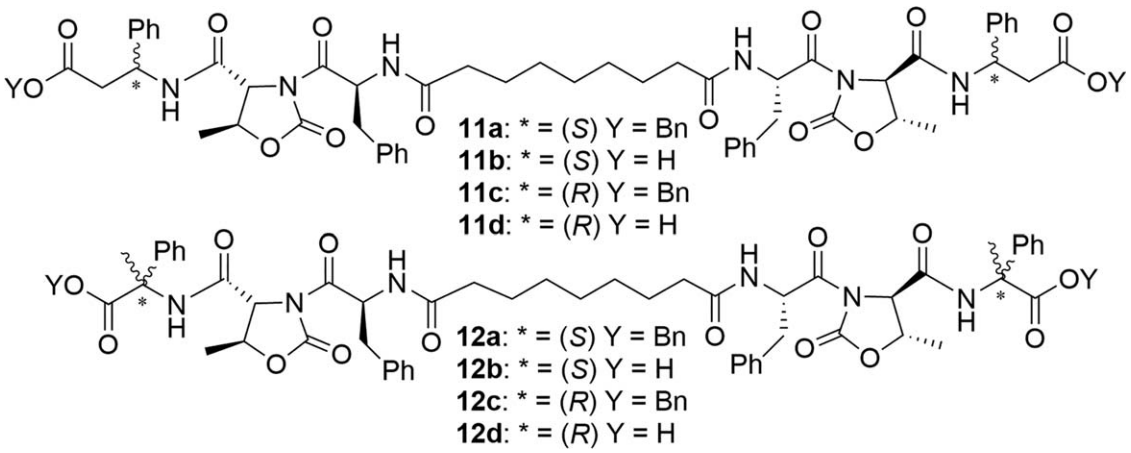

FIGURE 12 General molecular structure of bolaamphiphilic gelators

more compounds **10a–d** have been prepared, replacing the Oxd moiety with Pro units.

The propensity of all these compounds to form gels was checked. The samples were placed in a small test tube and dissolved in a suitable solvent in 10 mM concentration. Sonication was used to speed dissolution, by breaking intermolecular interactions, then the tubes were left stand still overnight. The most common diagnostic test of gelation is tube inversion: in this test, a sample tube containing the mixture of compound and solvent is inverted to ascertain if the sample would flow under its own weight (Figure 11). A gel is assumed to be a sample that has a yield stress that prevents it from flowing down the tube. Most compounds containing the L-Phe-D-Oxd moiety form gels, while the Pro-containing molecules never form gels in any condition, thus confirming that the Oxd moiety is required also for the gels formation, among this class of molecules.

Keeping this information in mind, the bolaamphiphilic derivatives **11a–d** and **12a–d** were prepared, to make gels with other solvents and in the presence of several metal ions (Figure 12).[44] These compounds are four benzyl esters and four carboxylic acids, all containing both a moiety of azelaic acid and four different pseudopeptides sharing the same skeleton (a phenyl group one atom apart from the oxazolidin-2-one carboxylic group): they form gels both as pure compounds and as stechiometric mixtures with metal ions. Very good results have been obtained with Zn(II) and Cu(II) ions, that form gels in several conditions, while the formation of gels in the presence of Cu (I), Al(III), and Mg(II) affords less satisfactory results.

3.2 | Fmoc containing LMWGs

Recently, the gelation behavior of Fmoc-protected dipeptides has been studied and reported.[45–49] A small library of 13

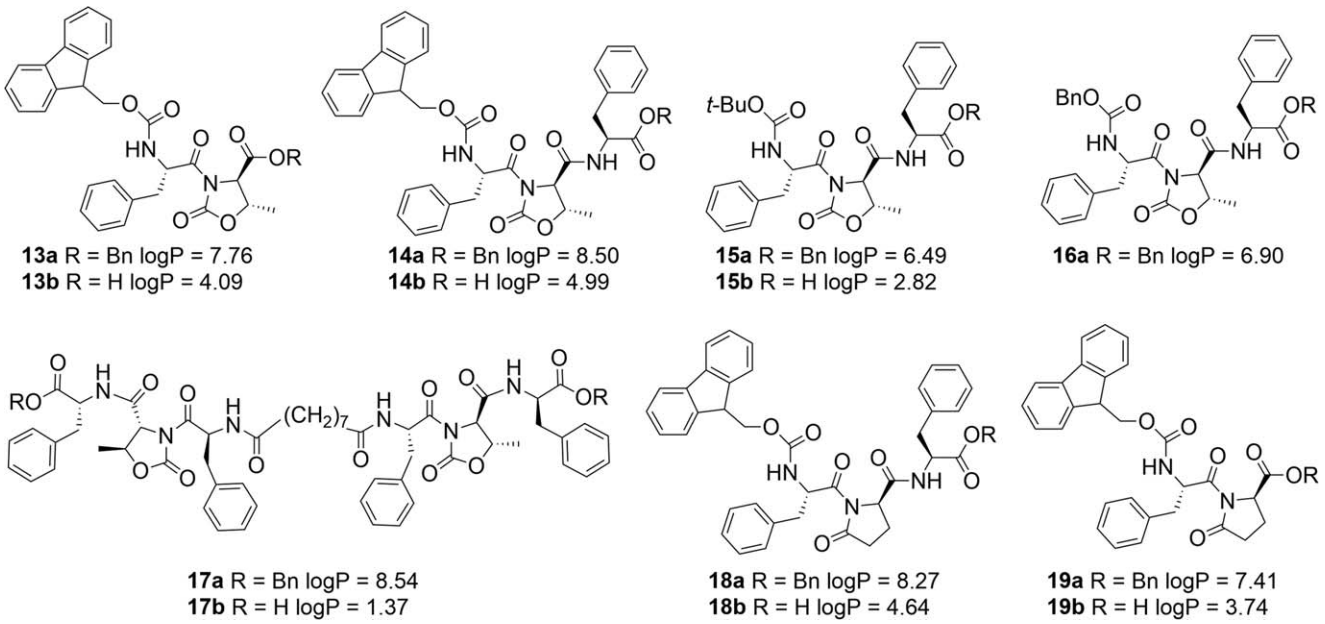

FIGURE 13 Molecular structure and log *P* values of *N*-protected pseudopeptides designed to gelate water and organic solvents

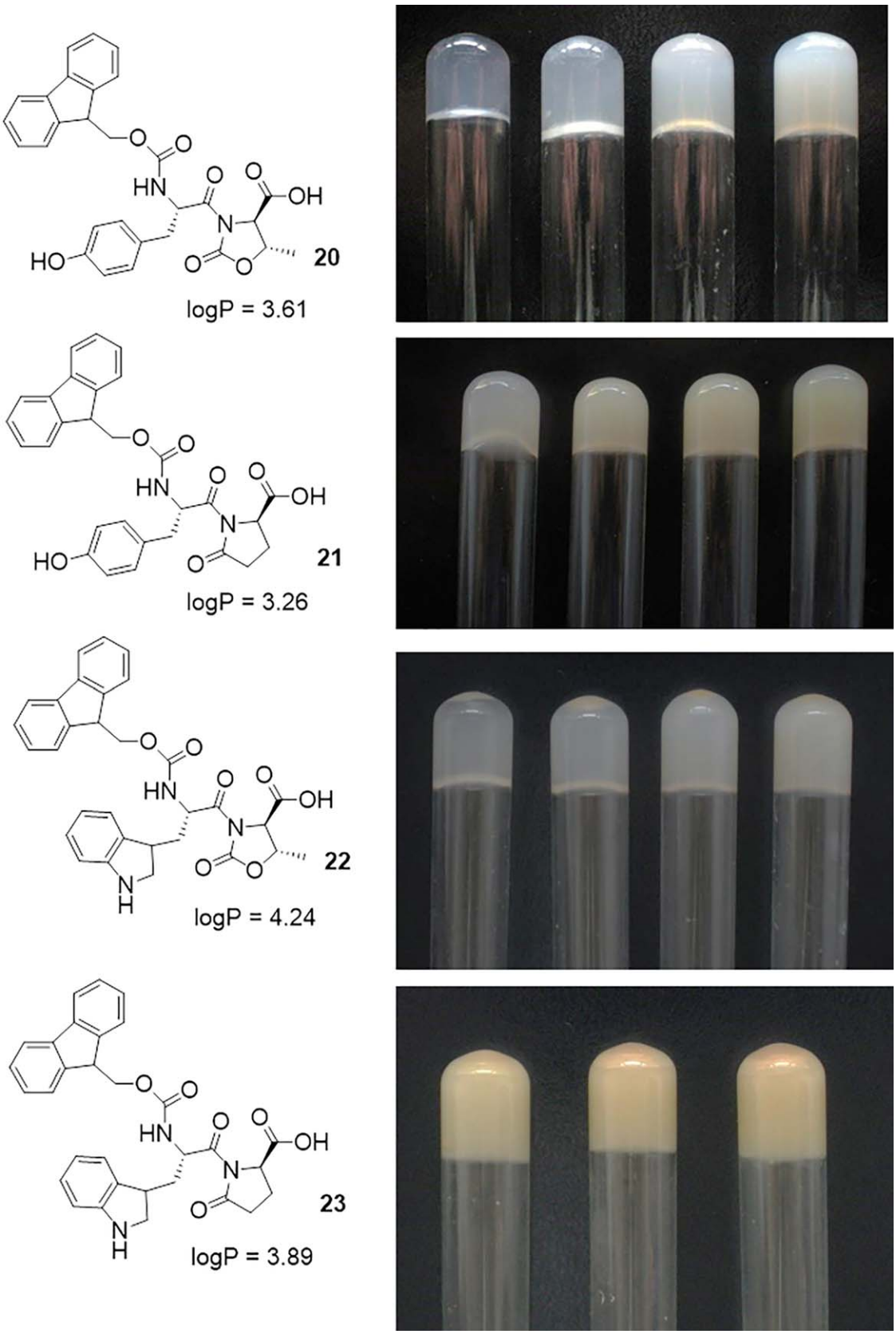

FIGURE 14 Photographs of hydrogels prepared in 0.5, 1.0, 1.5, and 2.0 concentrations in water (% w/w): (A) Fmoc-L-Tyr-D-Oxd-OH **20**; (B) Fmoc-L-Tyr-D-pGlu-OH **21**; (C) Fmoc-L-Trp-D-Oxd-OH **22**; (D) Fmoc-L-Trp-D-pGlu-OH **23**. Reproduced from Ref. 53 with permission from the American Chemical Society

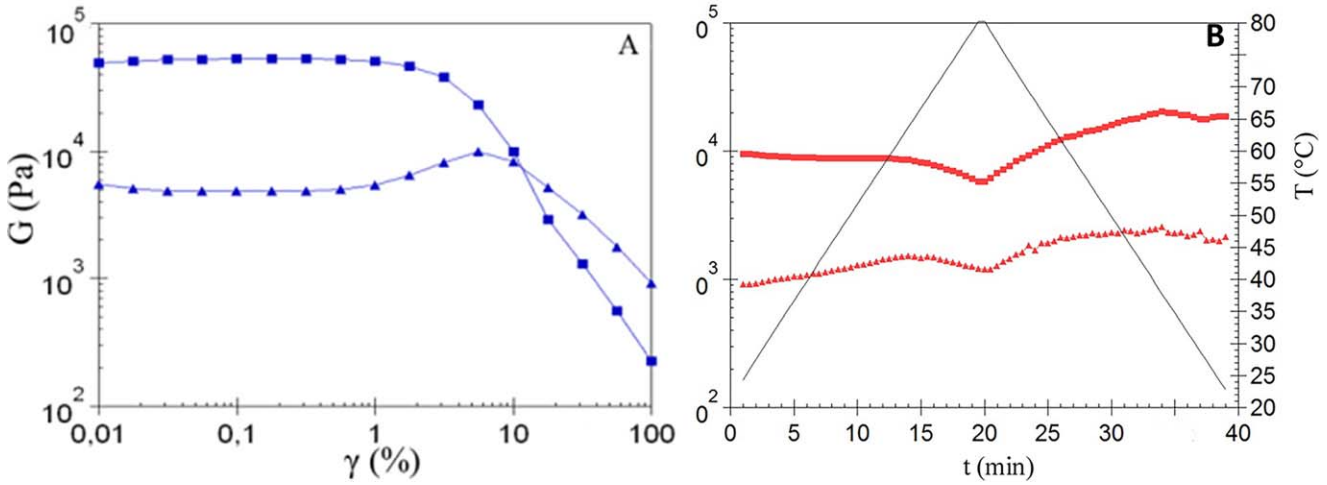

FIGURE 15 (A) Strain dependence of storage modulus (square) and loss modulus (triangle) at 2% w/w gelator concentration of Fmoc-L-Tyr-D-Oxd-OH **20**. The analyses were performed on the gels about 20 h after the gelation begun. (B) Temperature dependence of G' (squares) and G'' (triangles) for gels obtained from Fmoc-L-Tyr-D-Oxd-OH **20**. Continuous line represents the heating and cooling ramp. Reproduced from Ref. 53 with permission from the American Chemical Society

molecules containing either the L-Phe-D-Oxd core or the isosteric L-Phe-pGlu core (*p*Glu = pyroglutamic acid) is shown in Figure 13.[50] These molecules should behave as gelators able to form reversible gels with the phosphate-buffered saline (PBS), that is a buffer solution commonly used in biological research. In biomedicine, there is significant interest in exploiting self-assembly to construct mimics of the extracellular matrix (ECM) for cell-culture applications.[51]

The compounds have been all prepared in solution in excellent yields and have been tested as organogelators and/or hydrogelators in 10 mM concentration with a variety of solvents or solvent mixtures. Among them, only Fmoc-L-Phe-D-pGlu-OH **19b** is a hydrogelator that efficiently form gels with the phosphate-buffered saline (PBS 1×), hence it is an excellent candidate for the preparation of novel materials for applications such as drug release, biological assays, and tissue engineering. Moreover, Boc-L-Phe-D-Oxd-L-Phe-OBn **15a** is a good organogelator.

A rationale to explain the gelation behavior of these molecules takes into consideration their hydrophobicity expresses as log *P* (octanol/water partition coefficient), that is calculated as a sum of fragment-based contributions and correction factors.[52] Taking into consideration the log *P* values of all the compounds shown in Figure 13, an intermediate value of log *P* (about 6.5 for organogels and 3.5 for hydrogels) is a good starting point for the design of new LMWGs.

Four new LMWGs with a log *P* value that ranges between 3.26 and 4.24 have been prepared in multigram scale and their attitude to form hydrogels has been tested: Fmoc-L-Tyr-D-Oxd-OH **20**, Fmoc-L-Tyr-D-pGlu-OH **21**, Fmoc-L-Trp-D-Oxd-OH **22**, and Fmoc-L-Trp-D-pGlu-OH **23** (Figure 14).[53] All these compounds are good hydrogelators

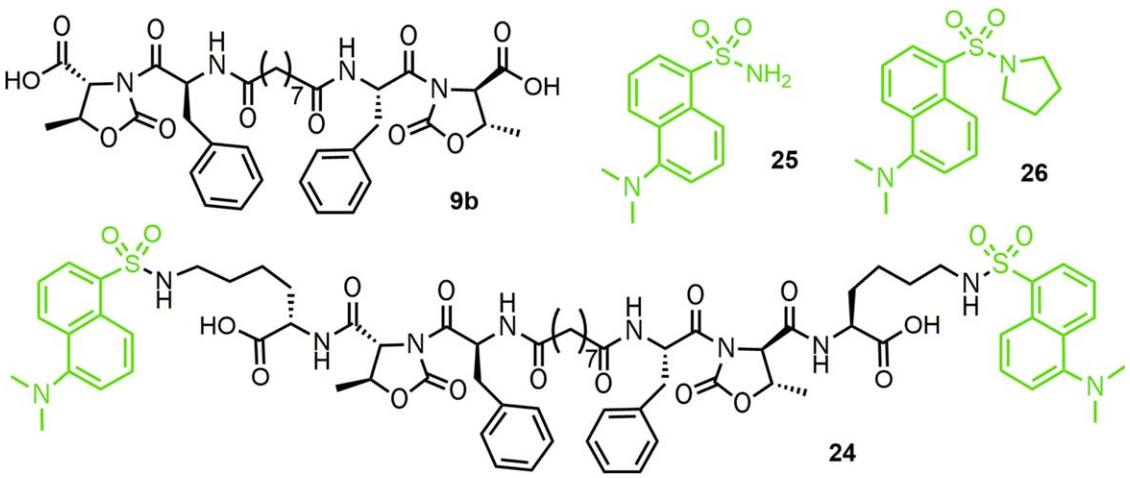

FIGURE 16 Chemical structure of compounds **9b**, **24, 25,** and **26**

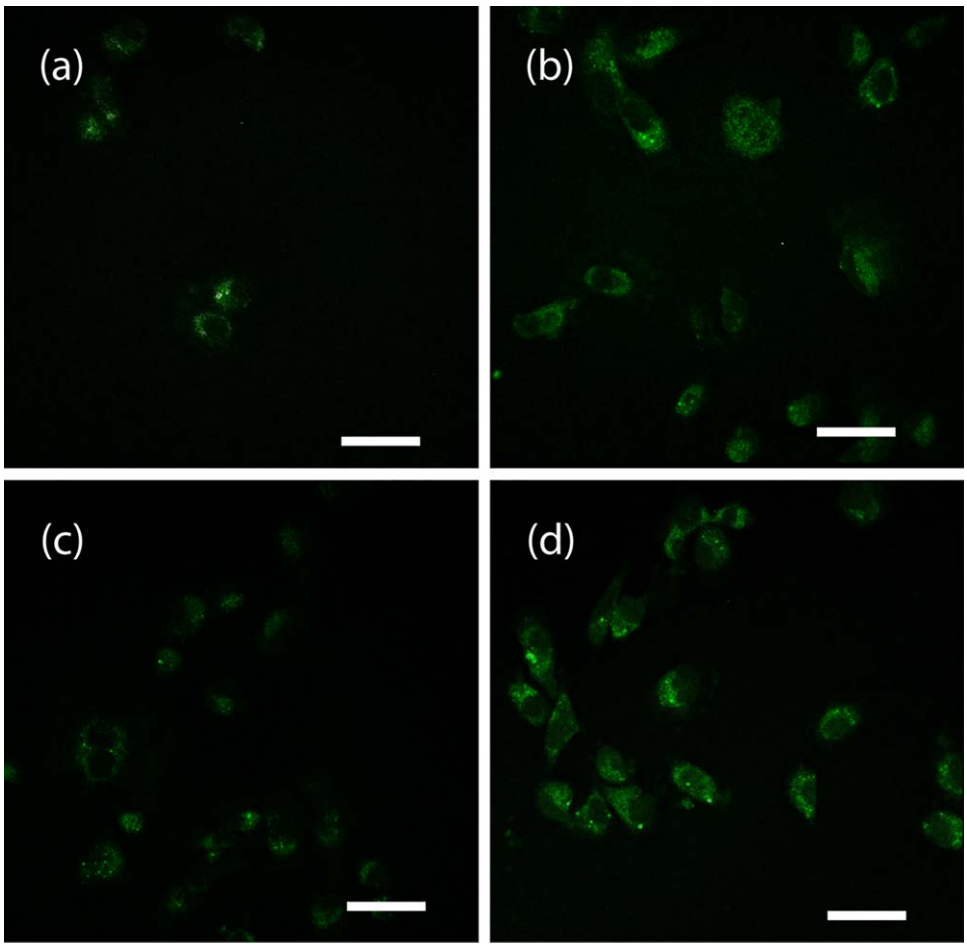

FIGURE 17 Confocal laser scanning micrographs of IGROV1 exposed to different hydrogels using **9b** as gelator, doped by little amount of the dansyl containing compounds **24**, **25,** and **26**. The dansyl group fluorescence is shown in green. Scale bar 50 μm. Reproduced from Ref. 55 with permission from the Beilstein Institute

when the gelation trigger is pH variation, obtained exploiting the slow hydrolysis of glucono-δ-lactone (GdL) added to a basic aqueous solution of the gelator.[54] The resulting gels are strong, transparent, and viscoelastic, as shown in Figure 14.

The gels have been characterized with several techniques: measurement of the melting point (Tgel) and of the viscoelastic properties, electronic circular dichroism (ECD), analysis of the transparency, and gelation time. Fmoc-L-Tyr-D-Oxd-OH **20** is an excellent gelator as UV–visible analysis demonstrated that it forms gels that possess high transparency, with a transmittance up to 25.6% at a wavelength of 600 nm.

Moreover, results of rheological experiments on the gel formed by **20** showed that the elastic response component (G') was approximately an order of magnitude larger than the viscous component (G'', loss modulus) in any case, indicating a "solid-like" attitude of the gels (Figure 15A). The thermal behavior of the gel formed by Fmoc-L-Tyr-D-Oxd-OH **20** was characterized performing an "ad-hoc" rheological temperature sweep experiment that is shown in Figure 15B. It indicates that G' is almost constant from 23°C up to about 65°C while G'', increased in the same temperature range. At higher temperatures, both G' and G'' values start to slightly decrease without displaying a crossover point. This result confirms that **20** forms a well-built and thermoreversible gel.

4 | APPLICATIONS

4.1 | Bolaamphiphilic LMWGs as Trojan horses

In Chapter we demonstrated that some bolamphiphiles of the series **11a–d** and **12a–d** efficiently gelate solutions containing metal ions.[44] Thus, if these materials are biocompatible, they may behave as "Trojan horses" and carry drug molecules into the cells.[55,56] To check the ability of these gels to cross the membrane barrier of ovarian cancer cells line IGROV-1 by confocal laser scanning microscopy, some fluorescent hydrogels have been prepared using the bolamphiphic gelator **9b** together with compounds 3.1, **24**, **25**, and **26**, all containing the fluorescent dansyl group (Figure 16).

Some images of confocal laser scanning micrographs of IGROV1 cells exposed to different hydrogels are shown in

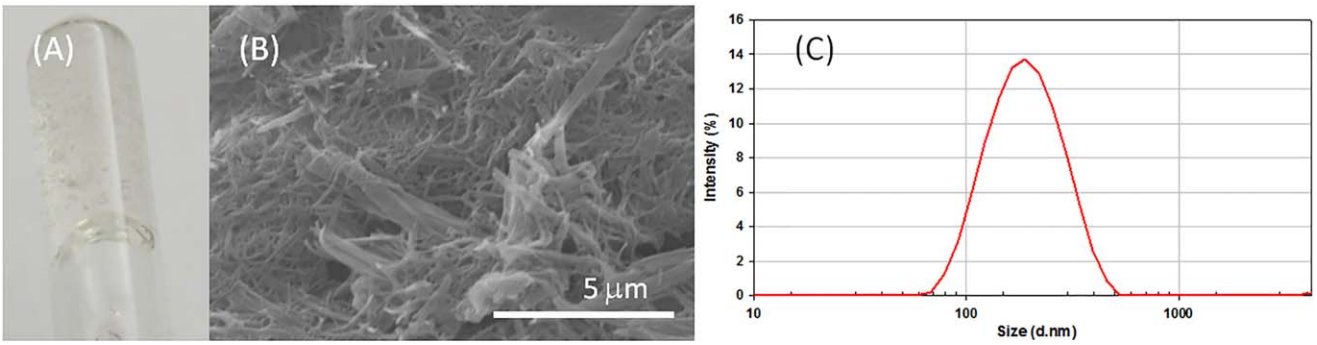

FIGURE 18 (A) Photograph of hydrogel obtained from a 10 mM solution of molecule $CH_2(C_3H_6CO$-L-Phe-D-Oxd-$OH)_2$ **9b** in a 10 mM $CaCl_2$ solution in 9:1 (*v*/*v*) mixture of H_2O/EtOH; (B) scanning electron microscopy picture of the corresponding xerogel. (C) Size distribution by volume of the particles from a 1 mM solution of molecule $CH_2(C_3H_6CO$-L-Phe-D-Pro-$OH)_2$ **10b** in a 10 mM $CaCl_2$ solution in 9:1 (*v*/*v*) mixture of H_2O/EtOH. Reproduced from Ref. 57 with permission from The Royal Society of Chemistry

Figure 17. These gels have been prepared using **9b** as gelator, doped with little amounts of **24**, **25**, or **26**.

The green fluorescence in the cytoplasm clearly demonstrate that all the hydrogels are internalized in IGROV-1 cells, thus the gels prepared with **9b** may behave as an excellent Trojan horse as they are biologically inactive, are internalized by cells and cargo on it molecules of different sizes.

4.2 | Shaping calcite crystals by bolamphiphilic LMWGs

We selected $CH_2(C_3H_6CO$-L-Phe-D-Oxd-$OH)_2$ **9b** that is an hydrogelator and $CH_2(C_3H_6CO$-L-Phe-D-Pro-$OH)_2$ **10b,** to compare their efficiency to shape calcite crystals.[57] As **10b** is soluble and does not promote the gel formation, its behavior was investigated by dynamic light scattering (DLS), that demonstrated that this molecule assembles in big structures having a diameter ranging from 100 nm to about 1 μm in 1 mM solution. In Figure 18C, the size distribution by volume of the particles from a 1 mM solution of **10b** in a 10 mM $CaCl_2$ solution in 9:1 (*v*/*v*) mixture of H_2O/EtOH is shown, together with picture of the hydrogel and of the xerogel formed by **9b** in the same experimental conditions.

Both **9b** and **10b** were used for $CaCO_3$ precipitation experiments without applying any filtration procedure. In Figure 19, some optical and scanning electron microscopy

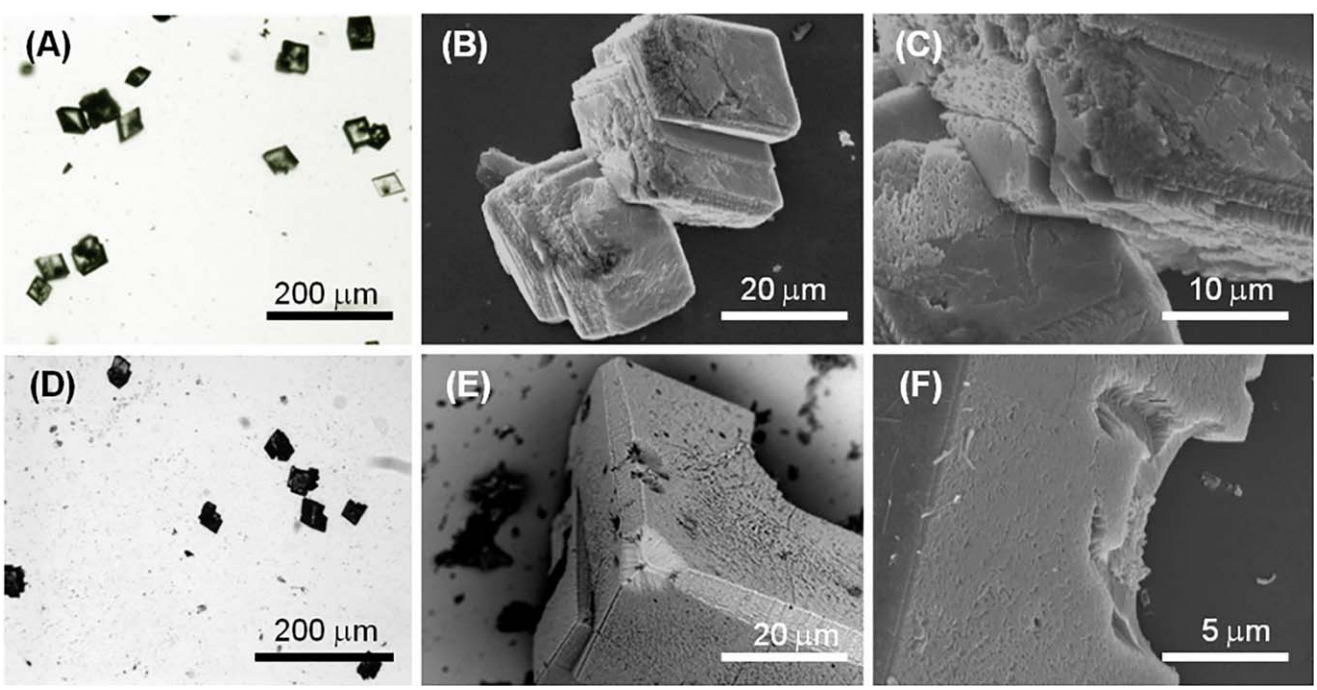

FIGURE 19 Optical (A, D) and scanning electron microscopy (B, C, E, F) pictures of calcite crystals precipitated from the 9/1 (v/*v*) H_2O/EtOH mixture in the presence of 10 mM **9b** (A–C) or **10b** (D–F). These pictures are representative of the entire population of crystals. Reproduced from Ref. 57 with permission from The Royal Society of Chemistry

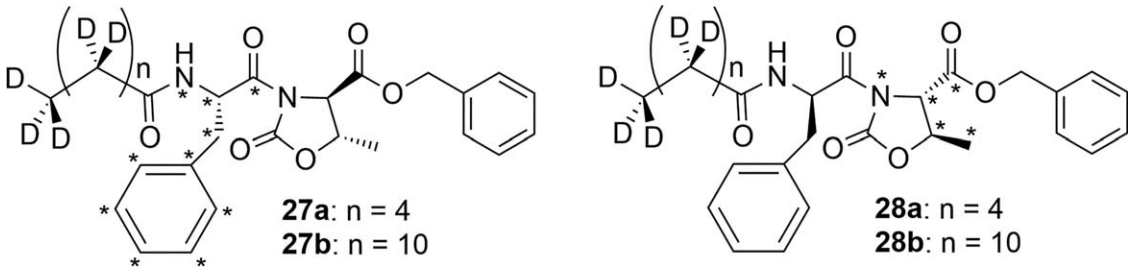

FIGURE 20 Molecular structure of the investigated lipopeptides in the different ^{13}C and ^{15}N labeled forms (labeled atoms are marked by asterisks)

pictures of calcite crystals precipitated from a H_2O/EtOH mixture in the presence of 10 mM **9b** or **10b** are shown. Both molecules are able to modify the shape of single crystals of calcite, but **9b** favors the formation of modified rhombohedral calcite showing new crystalline faces, while **10b** induced the formation of cavities and curvatures.

These two bolamphiphilic pseudopeptides diversely act as crystal growth modifiers, according to minor structural changes that mutate their self-assembling. As their physical state brings at a different space distribution of the interacting ionizable carboxylic groups, a diverse interaction with $CaCO_3$ is expected.[58] This outcome is in agreement with the behavior of some biomineralization proteins that are assumed to adopt an ordered conformation and geometry of ionizable functional groups, when they interact with biominerals.[59,60]

4.3 | Interaction of lipid derivatives of L-Phe-D-Oxd moiety with lipid membranes

In the final part of this survey, we describe the application of the L-Phe-D-Oxd derivatives **27a,b** and **28a,b**, that contain a lipid chain moiety coupled with the *N*-terminus (Figure 20).[61] Lipid modifications are known to play a decisive role in the formation of micelles, membranes, and other supramolecular structures due to the hydrophobic effect.[62]

We studied whether the self-assembly of the lipopeptides can be influenced by the presence of lipid membranes by means of solid-state NMR spectroscopy under magic-angle spinning (MAS) conditions, which has proven to successfully characterize peptide aggregates and membrane-associated peptides.[63] Addition of the *N*-terminal lipid modification did not cause a major disturbance of the structures these molecules form. The lipid modifications themselves showed highly rigid structures as inferred from solid-state ^2H NMR. The peptide backbone showed ^{13}C NMR chemical shifts in agreement with β-sheet secondary structures.

As addition of a lipid modification to the *N*-terminus is a common motif in biology to attach proteins to the membrane,[64] the lipopeptides **27a,b** and **28a,b** were investigated in the presence of synthetic phospholipid (POPC) bilayers. Two different molecular species were detected under these circumstances: (*i*) lipopeptide monomers that showed chain order parameters similar to those of the host membrane and (*ii*) lipopeptide aggregates that exhibited very similar structures and dynamics as the crystalline aggregates (Figure 21). Only part of the peptide aggregates are dissolved in the membrane and will most likely occur in a monomeric form.

Overall, the study showed that the general molecular architecture of peptides comprising the building block L-Phe-D-Oxd is not altered by *N*-terminal lipid modifications if investigated in the crystalline state. However, in the presence

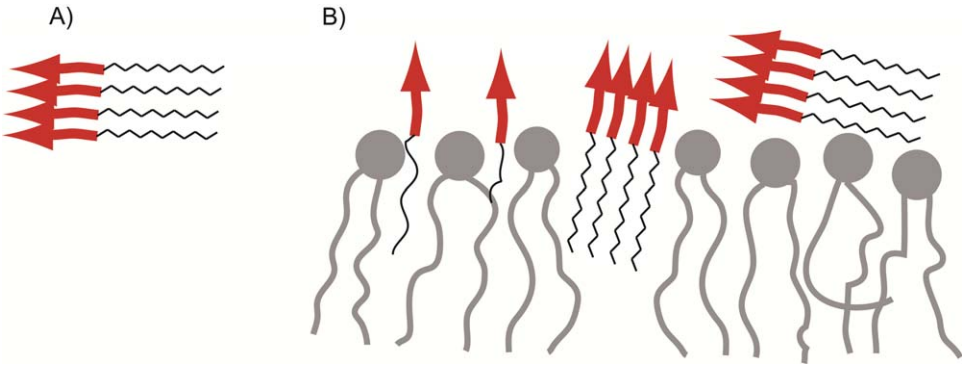

FIGURE 21 This cartoon summarizes that (A) in the absence of membranes, lipopeptides form highly ordered β-sheet like nanofibers with the lipid modifications in a rigid all *trans* conformation; (B) when lipid membranes are present, larger peptide aggregates can bind to the membrane surface or insert into the membrane, but also dissociate and insert into the membrane as monomers. Reproduced from Ref. 61 with permission from The Royal Society of Chemistry

of lipid membranes, the nanofibered structure only partially prevails, as the molecules can also disaggregate and be immersed in the lipid membrane as many lipidated proteins and peptides do.

5 | CONCLUSIONS

In this article, we demonstrated that L-Phe-D-Oxd moiety may be considered as a privileged scaffold for the formation of supramolecular materials, due to its tendency to aggregate in fibers regardless the substituents both at the *N*-terminus and at the *C*-terminus. The presence of the Oxd moiety is essential for the material formation: when Oxd is replaced with Pro, only liquids or amorphous solids are obtained.

Starting from Boc-L-Phe-D-Oxd-OBn **1** that gets organized into a very stable fiber-like material, several derivatives have been described: they may form either materials organized in β-sheets or in supramolecular helices. For instance, lipidated derivatives containing the L-Phe-D-Oxd moiety form fibers that effectively interact with lipid membrane.

Some derivatives of the L-Phe-D-Oxd moiety are LMWGs as they promote the formation of organogel and hydrogels. These LMWGs may be divided into two families according to the side chain structure: either bolamphiphilic gelators or Fmoc-derived gelators. Rheological studies demonstrated that these materials are very strong gels with interesting viscoelastic and thermoreversible properties.

These LMWGs may form both organogels and hydrogels, useful for several applications: metal containing gels, liposomes capable of affecting the growth of calcite crystals and Trojan horses able to carry organic compounds into the cells. These hydrogelators may represent a new tool for the controlled release of drugs into specific cells, as they are (i) responsive to external stimuli, (ii) not toxic and able to be internalized by cell, and (iii) easy to functionalize to be targeted into different substrates. The formation of self-assembled gels containing anticancer agents, such as platinum(II)-based anticancer agents could furnish an innovative answer to the problem of delivery of these compounds, reducing their high toxicity toward "normal" tissues.

REFERENCES

[1] H. Yang, S. Y. Fung, M. Pritzker, P. Chen, Angew. Chem. - Int. Ed. 2008, 47, 4397.

[2] M. Guthold, W. Liu, E. A. Sparks, L. M. Jawerth, L. Peng, M. Falvo, R. Superfine, R. R. Hantgan, S. T. Lord, Cell Biochem. Biophys. 2007, 49, 165.

[3] T. Scheibel, Curr. Opin. Biotechnol. 2005, 16, 427.

[4] I. Morgado, M. Fändrich, Curr. Opin. Colloid Interface Sci. 2011, 16, 508.

[5] J. A. Hebda, I. Saraogi, M. Magzoub, A. D. Hamilton, A. D. Miranker, Chem. Biol. 2009, 16, 943.

[6] P. P. Hu, C. Z. Huang, Acta Biochim. Biophys. Sin. 2013, 45, 435.

[7] A. Tahiri-Alaoui, M. Bouchard, J. Zurdo, W. James, Protein Sci. 2003, 12, 600.

[8] F. O. Bastian, J. Neuropathol. Exp. Neurol. 2014, 73, 104.

[9] W. H. Binder, O. W. Smrzka, Angew. Chem. - Int. Ed. 2006, 45, 7324.

[10] A. Perczel, P. Hudaky, V. K. Palfi, J. Am. Chem. Soc. 2007, 129, 14959.

[11] S. Guha, M. G. B. Drew, A. Banerjee, Chem. Mater. 2008, 20, 2282.

[12] S. K. Maji, D. Haldar, A. Banerjee, A. Banerjee, Tetrahedron 2002, 58, 8695.

[13] S. K. Maji, M. G. Drew, A. Banerjee, Chem. Commun. 2001, 1946.

[14] R. V. Ulijn, A. M. Smith, Chem. Soc. Rev. 2008, 37, 664.

[15] F. Rúa, S. Boussert, T. Parella, I. Díez-Pérez, V. Branchadell, E. Giralt, R. M. Ortuño, Org. Lett. 2007, 9, 3643.

[16] T. A. Martinek, A. Hetényi, L. Fulop, I. M. Mándity, G. K. Tóth, I. Dékány, F. Fülöp, Angew. Chem. - Int. Ed. 2006, 45, 2396.

[17] F. E. Cohen, J. W. Kelly, Nature 2003, 426, 905.

[18] J. Sato, T. Takahashi, H. Oshima, S. Matsumura, H. Mihara, Chemistry 2007, 13, 7745.

[19] R. Mishra, B. Bulic, D. Sellin, S. Jha, H. Waldmann, R. Winter, Angew. Chem. - Int. Ed. 2008, 47, 4679.

[20] I. Cherny, E. Gazit, Angew. Chem. - Int. Ed. 2008, 47, 4062.

[21] S. Lucarini, C. Tomasini, J. Org. Chem. 2001, 66, 727.

[22] C. Tomasini, V. Trigari, S. Lucarini, F. Bernardi, M. Garavelli, C. Peggion, F. Formaggio, C. Toniolo, Eur. J. Org. Chem. 2003, 4, 259.

[23] G. Angelici, G. Luppi, B. Kaptein, Q. B. Broxterman, H. J. Hofmann, C. Tomasini, Eur. J. Org. Chem. 2007, 2713.

[24] S. Kakinoki, Y. Hirano, M. Oka, Pept. Sci. 2004, 453.

[25] S. Kakinoki, Y. Hirano, M. Oka, Pept. Sci. 2004, 457.

[26] L. Garbuio, B. Lewandowski, P. Wilhelm, L. Ziegler, M. Yulikov, H. Wennemers, G. Jeschke, Chemistry 2015, 21, 10747.

[27] M. V. Sonar, K. N. Ganesh, Org. Lett. 2010, 12, 5390.

[28] N. Zanna, L. Milli, B. Del Secco, C. Tomasini, Org. Lett. 2016, 18, 1662.

[29] G. Angelici, G. Falini, H. J. Hofmann, D. Huster, M. Monari, C. Tomasini, Angew. Chem. Int. Ed. 2008, 47, 8075.

[30] G. Angelici, G. Falini, H. J. Hofmann, D. Huster, M. Monari, C. Tomasini, Chemistry 2009, 15, 8037.

[31] N. Castellucci, G. Falini, L. Milli, M. Monari, S. Abbate, G. Longhi, E. Castiglioni, G. Mazzeo, C. Tomasini, Chempluschem 2014, 79, 114.

[32] N. Castellucci, G. Angelici, G. Falini, M. Monari, C. Tomasini, Eur. J. Org. Chem. 2011, 3082.

[33] M. Reches, E. Gazit, Nat. Nanotechnol. 2006, 1, 195.

[34] G. Angelici, N. Castellucci, G. Falini, D. Huster, M. Monari, C. Tomasini, Cryst. Growth Des. 2010, 10, 923.

[35] K. Kodama, Y. Kobayashi, K. Saigo, Cryst. Growth Des. 2007, 7, 935.

[36] R. G. Weiss, J. Am. Chem. Soc. 2014, 136, 7519.

[37] X. Du, J. Zhou, J. Shi, B. Xu, Chem. Rev. 2015, 115, 13165.

[38] M. T. Cation, A. Schrey, A. Vescovi, A. Knoll, C. Rickert, U. Koert, Angew. Chem.-Int. Ed. 2000, 39, 900.

[39] S. Fleming, R. V. Ulijn, Chem. Soc. Rev. 2014, 43, 8150.

[40] A. Dasgupta, J. H. Mondal, D. Das, RSC Adv. 2013, 3, 9117.

[41] D. K. Smith, Chem. Soc. Rev. 2009, 38, 684.

[42] P. Curcio, F. Allix, G. Pickaert, B. Jamart-Grégoire, Chemistry 2011, 17, 13603.

[43] T. Shimizu, Macromol. Rapid Commun. 2002, 23, 311.

[44] N. Castellucci, G. Falini, G. Angelici, C. Tomasini, Amino Acids 2011, 41, 609.

[45] K. L. Morris, L. Chen, A. Rodger, D. J. Adams, L. C. Serpell, Soft Matter 2015, 11, 1174.

[46] G. Fichman, E. Gazit, Acta Biomater. 2014, 10, 1671.

[47] B. Adhikari, J. Nanda, A. Banerjee, Chemistry 2011, 17, 11488.

[48] D. J. Adams, M. F. Butler, W. J. Frith, M. Kirkland, L. Mullen, Soft Matter, 2009, 5, 1856–1862.

[49] L. Chen, K. Morris, A. Laybourn, D. Elias, M. R. Hicks, A. Rodger, L. Serpell, D. J. Adams, Langmuir 2010, 26, 5232.

[50] L. Milli, N. Castellucci, C. Tomasini, Eur. J. Org. Chem. 2014, 2014, 5954.

[51] V. Jayawarna, M. Ali, T. A. Jowitt, A. F. Miller, A. Saiani, J. E. Gough, R. V. Ulijn, Adv. Mater. 2006, 18, 611.

[52] D. J. Adams, L. M. Mullen, M. Berta, L. Chen, W. J. Frith, Soft Matter 2010, 6, 1971.

[53] N. Zanna, A. Merlettini, G. Tatulli, L. Milli, M. L. Focarete, C. Tomasini, Langmuir 2015, 31, 12240.

[54] D. J. Adams, M. F. Butler, W. J. Frith, M. Kirkland, L. Mullen, P. Sanderson, Soft Matter 2009, 5, 1856.

[55] N. Castellucci, G. Sartor, N. Calonghi, C. Parolin, G. Falini, C. Tomasini, Beilstein J. Org. Chem. 2013, 9, 417.

[56] C. Martin, E. Oyen, J. Mangelschots, M. Bibian, T. Ben Haddou, J. Andrade, J. Gardiner, B. Van Mele, A. Madder, R. Hoogenboom, M. Spetea, S. Ballet, Med. Chem. Commun. 2016, 7, 542.

[57] C. Tomasini, N. Castellucci, V. C. Caputo, L. Milli, G. Battistelli, S. Fermani, G. Falini, CrystEngComm 2015, 17, 116.

[58] M. Lahav, L. Addadi, L. Leiserowitz, Proc. Natl. Acad. Sci. USA 1987, 84, 4737.

[59] A. Adamiano, S. Bonacchi, N. Calonghi, D. Fabbri, G. Falini, S. Fermani, D. Genovese, D. Kralj, M. Montalti, B. Njegić Džakula, *et al*. Chemistry 2012, 18, 14367.

[60] J. S. Evans, Chem. Rev 2008, 108, 4455.

[61] H. Scheidt, A. Sickert, T. Meier, N. Castellucci, C. Tomasini, D. Huster, Org. Biomol. Chem. 2011, 9, 6998.

[62] N. T. Southall, K. A. Dill, A. D. J. Haymet, J. Phys. Chem. 2002, 106, 521.

[63] H. A. Scheidt, I. Morgado, S. Rothemund, D. Huster, M. Fändrich, Angew. Chem. - Int. Ed. 2011, 50, 2837.

[64] L. Brunsveld, H. Waldmann, D. Huster, Biochim. Biophys. Acta – Biomembr. 2009, 1788, 273.

How to cite this article: Tomasini C and Zanna N. Oxazolidinone-containing pseudopeptides: supramolecular materials, fibers, crystals, and gels. *Peptide Science* 2017;108:e22898. https://doi.org/10.1002/bip.22898